



REGULAR ARTICLE

A Medical Image-Based Computational Framework for Electromagnetic Field Mapping and SAR Estimation in Biological Tissues

S. Chandrappa<sup>1</sup>, Prithviraj<sup>2,\*</sup>, I.S. Rajesh<sup>3,†</sup>, K. Madhusudhana<sup>4</sup>, K.R. Sharath<sup>5</sup>, A. Pai<sup>6</sup>

<sup>1</sup> Department of Computer Science and Engineering (Data Science), Nagarjuna College of Engineering and Technology, Beedaganahalli Post, Devanahalli, Venkatagiri Kote, Bengaluru, India

<sup>2</sup> Department of Computer Science and Engineering, Nitte (Deemed to be University), NMAM Institute of Technology, Nitte, Karkala, India

<sup>3</sup> Department of Artificial Intelligence and Machine Learning, BMS Institute of Technology and Management, Bengaluru, India

<sup>4</sup> Department of Electronics & Communication Engineering, SDM Institute of Technology, Ujire, India

<sup>5</sup> Department of Computer Science and Engineering, Graphic Era (Deemed to be University), Dehradun, India

<sup>6</sup> MIT – School of Computing, MIT Art, Design and Technology University, Pune, Maharashtra, India

(Received 03 January 2026; revised manuscript received 22 April 2026; published online 29 April 2026)

It is widely accepted from the universe that magnetic radiation has a vital role to play in the field of medical imaging, such as Magnetic Resonance Imaging (MRI), where radiofrequency electromagnetic fields emitted from the medical instruments interact with tissues of biological objects near the devices. In this research work, a problem caused by the Electromagnetic fields and an image-based approach is presented to calculate and evaluate electromagnetic field disseminations using medical images obtained using a triangulation technique. An examination of brain MRI images collected from the publicly available dataset was accomplished and normalized fields of electromagnetic intensity maps were created using the data. Based on the information present in those maps, the RF magnetic field distributions, electric fields, power densities, and specific absorption rates (SARs) were calculated. Later, an examination based on thresholds was engaged to find the regions with high magnetic fields. Results obtained from the research work establish that the exposure to electromagnetic fields in biological tissues is spatially non-uniform, with certain regions demonstrating higher levels of flux and energy absorption. It is important to note that, even though the values obtained from the data are representing relative measurements, they are reliable with known electromagnetic field behavior observed in biological tissues. As a result of the proposed methodology, a practical and operative structure for evaluating and estimating radiation exposure in medical imaging environments is provided.

**Keywords:** Electromagnetic fields, Optical radiation, MRI, SAR, Biological effects, Medical imaging.

DOI: [10.21272/jnep.18\(2\).02005](https://doi.org/10.21272/jnep.18(2).02005)

PACS numbers: 87.19.lf, 87.50.Y-, 87.80.Lg

1. INTRODUCTION

Quantum Electromagnetic fields (EMFs) are everywhere in environment, mainly due to the electric current. Physical and biological objects can encounter EMFs in various activities. These include industrial processes like electrolysis, welding, sealing, broadcasting, and electricity generation. They also exist in medical processes such as Magnetic Resonance Imaging (MRI). The health effects of overexposure can vary based on the intensity and distance from the sources. In our daily lives, we expose to fields ranging from the static magnetic field to high-frequency fields from communication devices like mobile phones and their base stations, as shown in figure 1. For low-frequency fields from sources like power lines or welding equipment, we need to distinguish among the electric and magnetic fields. However, for fields with frequencies in the MHz range or higher, there is a

consistent relationship between the fields.

The electric field ( $E$ ) is formed when two points have a voltage difference between them, and a current flows between them. When current flows through materials, a magnetic field ( $B$ ) is created as a result. The electric field is measured in volts per meter, or  $V/m$ , whereas the magnetic field is sometimes expressed as flux density, or Tesla ( $T$ ). In both cases,  $E$  and  $B$  can be seen as vector quantities, which means that they have both magnitude and direction. According to Fig. 1, fields are often represented by field lines, which can be seen in the figure below. The  $E$  field is always characterized by the start point of a positive charge and the end point of a negative charge.  $B$  fields form closed loops, meaning that there is no beginning or an end to the loops.

The health effects of overexposure can vary based on the intensity and distance from EMF sources, as well as the type of electromagnetic radiation, such as

\* Correspondence e-mail: [prithvijain28@gmail.com](mailto:prithvijain28@gmail.com)

† [is.rajesh081@gmail.com](mailto:is.rajesh081@gmail.com)



its frequency or wavelength. Acute symptoms are clearly defined. In the high frequency range, like broadcasting and radars, severe burns can happen. In the low frequency range, such as welding and electricity production and distribution, induced currents can impact the central or peripheral nervous system. People exposed to low frequencies may also experience vertigo, nausea, a metallic taste, and magnetophosphenes, or flashes in the eyes. In very rare cases, significant indirect safety issues can arise when strong magnets pull a ferromagnetic object, causing it to hit someone accidentally positioned between the magnet and the metallic object.

When human or biological objects exposed to low-frequency electric or magnetic fields, electrical currents are generated in their bodies. If the current is large compared to object can resist enough, there is a risk of electric shock, similar to touching a live wire. Induced currents at the head and trunk affect the central nervous system at frequencies up to 10 MHz.

The current in the body flows along different paths and with varying strengths, depending on the orientation of the field. This is typically described by the amount of energy absorbed per unit time and mass, known as the Specific Absorption Rate (SAR), measured in watts per kilogram (W/kg). For mobile phone use, the exposure limit is defined in SAR. Most of phones comply with this directive; there is no need to measure electromagnetic fields (EMFs) from phones.

Pophof et al. discussed the biological effects of electric and electromagnetic fields on animals and plants. They identified how these interactions work but did not provide numerical EMF distribution within tissues [1]. Oladipo et al. reviewed electromagnetic radiation impacts on human reproductive health, emphasizing biochemical damage, yet lacked computational or image-based field visualization methods [2]. Zheng et al. examined behavioral effects of 2650 MHz EMR on mice and reported minor memory influence, but did not map internal SAR or field patterns in brain tissues [3]. Srinivas et al. investigated radiation interactions with physical and biological systems and established exposure limits, while Chandrappa et al. proposed artifact-reduction methods in medical imaging; however, both studies did not address direct extraction of EMF or SAR distributions from MRI images [4, 5]. These limitations highlight the need for an image-based computational framework for spatial EMF exposure analysis.

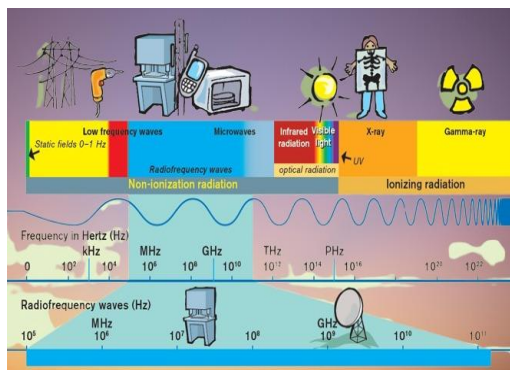


Fig. 1 – A schematic drawing of the electromagnetic spectrum

Table 1 encompasses some of the common areas and workplaces where there is a possible risk of exposure to EMFs in various frequencies. It is important record different work activities near specific EMF sources can lead to various exposure patterns.

Table 1 – Workplaces with low, medium, or high risk for interference

| Workplace/Occupation                                | EMF level |        |      |
|---|-----------|--------|------|
|   | Low       | Medium | High |
| An office environment                               | x         |        |      |
| The Shop  | x         |        |      |
| A home-based daycare service and a cleaning service | x         |        |      |
| The Library   |           | x      |      |
| Electric truck driving area                         |           | x      |      |
| Engine driving area                                 |           | x      |      |
| The kitchen of a restaurant (induction hubs)        |           | x      |      |
| Workers on the roof (at the base station)           |           | x      | x    |
| Glue drying   |           |        |      |
| Heat is generated by induction                      |           |        | x    |
| Work carried out on MRI machines                    |           |        | x    |
| Work in the TMS field                               |           |        | x    |
| Welding with electricity                            |           |        | x    |
| Welding of plastic materials                        |           |        | x    |
| In the field of surgery, diathermy is used          |           |        | x    |
| Electrolytic cells                                  |           |        | x    |
| Industries involving heavy machinery                |           |        | x    |
| In the field of energy production/distribution      |           |        | x    |

When a person or biological object is exposed to a magnetic field, it causes currents to form in the body. The current will flow in different paths and with varying strengths based on the orientation of the field, as shown in Fig. 2(a). According to Fig. 2(b), when RF energy is reflected to the body, it can be absorbed as a result of the absorption. The Specific Absorption Rate (SAR) of the substance is commonly described as the amount of energy that can be absorbed per unit of time and mass in what is known as watts per kilogram (W/kg). In the specific case of using a mobile phone for long durations of time, the exposure limit is measured in SARs. Some phones have SAR values near the upper limit, though still legal but danger to human organs.

Motivated by the need for practical and accessible electromagnetic exposure assessment [6-9], this work presents an image-based approach for analyzing electromagnetic field distributions from medical images. By processing colorized brain MRI data, relative electromagnetic field intensity, induced electric field,

power density, and specific absorption rate are estimated. The proposed methodology enables visualization of spatial exposure patterns and identification of localized high-field regions, providing a useful framework for preliminary safety analysis in medical imaging environments.

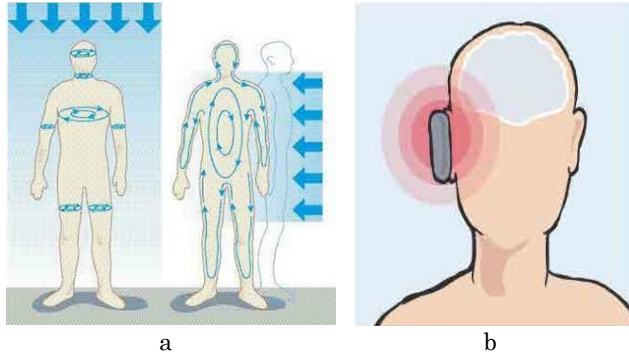


**Fig. 2** – Human exposure to electromagnetic fields (EMF) from external radiation sources (a). RF energy absorption in the human head during mobile phone use (SAR effect) (b)

The current work is important because it presents a computational image-based framework for estimating and visualizing electromagnetic field (EMF), electric field, power density, and specific absorption rate (SAR) distributions from MRI images. A new approach has been established to measure EMF exposure directly from medical image data, instead of using physical probes or complicated numerical solvers as in traditional EMF exposure studies. As a result, it is possible to find the location of localized high-field regions (hotspots) within biological tissues in a visual way. The proposed system provides a cost-effective and accessible process for measuring EMF exposure and supporting safety awareness in medical imaging settings. This proposed framework combines electromagnetics and medical imaging. This will provide a solid foundation for future quantitative dosimetry and research on bio electromagnetic safety.

## 2. METHODOLOGY

In this work, electromagnetic field measurement is performed using colorized brain MRI images obtained from a publicly available dataset. The study focuses on extracting relative RF EMF distributions and estimating associated safety-related parameters through image-based analysis. The dataset used for this study is from Kaggle: Brain Tumor (MRI) Detection Colorized. The overall methodology for electromagnetic field measurement from medical images follows a systematic image-based analytical pipeline, as shown in Fig. 3:

### 2.1 Input RF EMF Heatmap Acquisition

A colorized brain MRI image representing RF electromagnetic field intensity distribution is used as input. Each pixel color corresponds to a relative field magnitude.

### 2.2 Image Pre-processing

The input image is changed into a grayscale intensity map. The grayscale intensity is assumed to be proportional to the relative electromagnetic field strength at each spatial location.

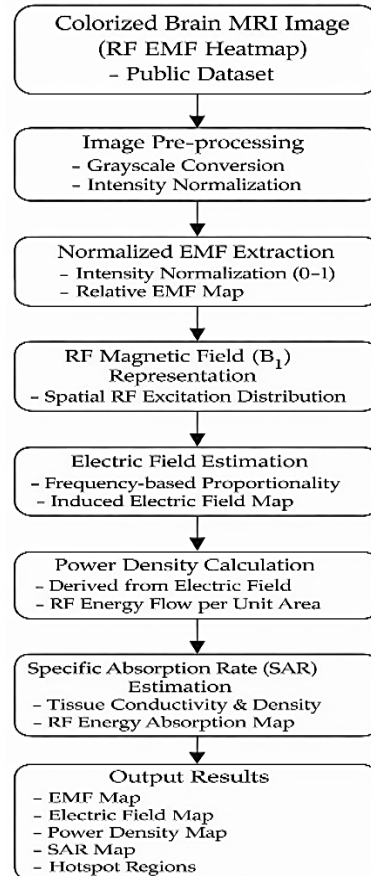


**Fig. 3** – Image-based workflow for electromagnetic field measurement and safety parameter estimation from colorized brain MRI images

### 2.3 Normalized EMF Extraction

The grayscale image is normalized to a range of 0 to 1 to obtain a normalized EMF map. This normalized representation provides relative electromagnetic field intensity without requiring hardware-level calibration.

### 2.4 RF Magnetic Field ( $B$ ) Representation

The normalized EMF map is interpreted as a relative RF magnetic field ( $B$ ) distribution, which represents the spatial variation of the RF excitation field in MRI.

### 2.5 Electric Field Estimation

The RF electric field is estimated from the relative  $B$  field using frequency-based proportionality. Although simplified, this estimation shows meaningful changes in the induced electric fields within biological tissues.

### 2.6 Power Density Calculation

Power density comes from the estimated electric field based on relationships in electromagnetic waves. This measure shows the flow of RF energy per unit area.

### 2.7 SAR Estimation

Specific Absorption Rate (SAR) is calculated based on assumptions about tissue conductivity and density. SAR gives information about how RF energy is absorbed in tissues and is an important safety measure for MRI.

### 2.8 Hotspot Detection

High-EMF regions are found by setting a threshold on the normalized EMF map. These hotspots show specific areas where the electromagnetic field intensity is high.

## 3. RESULTS AND DISCUSSION

This section presents the results from the image-based electromagnetic field analysis of colorized brain MRI data. The extracted outputs include normalized electromagnetic field intensity, estimated electric field, power density, specific absorption rate (SAR), and identified high-field hotspot regions.

The normalized EMF map shows how the electromagnetic field intensity is distributed throughout the brain. When compare it to the input RF EMF heat map, normalization improves the contrast and highlights specific areas with higher field intensity.

The estimated electric field map shows how induced electric fields vary in biological tissue based on RF exposure. The estimated SAR map shows patterns of RF energy absorption, with higher values found in certain areas.

The power density distribution shows areas where RF energy spreads more within brain tissue. This reflects differences in how electromagnetic energy flows in space.

High-EMF hotspot regions were found by setting a threshold on the normalized EMF map. This showed specific areas with higher electromagnetic field intensity.

Table 2 illustrates the Summary of electromagnetic field and SAR values from MRI analysis. The results

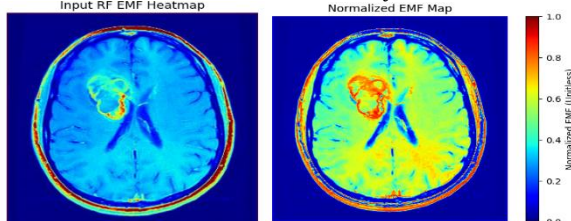


Fig. 4 – Input RF EMF heatmap and the corresponding normalized electromagnetic field (EMF) intensity map created from a colorized brain MRI image

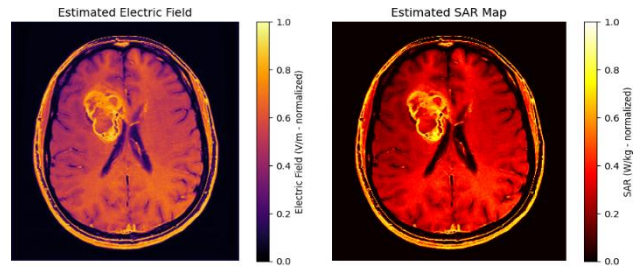


Fig. 5 – Estimated electric field distribution and normalized specific absorption rate (SAR) map derived from the relative RF magnetic field

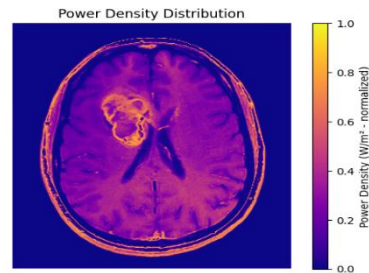


Fig. 6 – Power density distribution showing RF energy flow per unit area within biological tissue

Table 2 — Numerical Summary

| Parameter                | Value |
|--------------------------|-------|
| Maximum EMF              | 1.000 |
| Mean EMF                 | 0.297 |
| Maximum SAR (normalized) | 1.000 |
| Mean SAR (normalized)    | 0.162 |

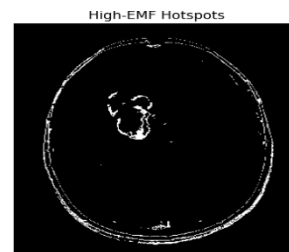


Fig. 7 – High-EMF hotspot regions identified using a threshold-based analysis of the normalized EMF map

show that exposure to electromagnetic fields in biological tissues is uneven. There are specific areas that have higher field intensity and energy absorption. Even though the extracted values are normalized and indicate relative measurements, the spatial patterns we observed match the known behavior of electromagnetic fields in biological tissues.

## 4. CONCLUSION

This study showed how to measure and analyze electromagnetic fields from medical images using an image-based computational method. The results of proposed system analysis were obtained by normalizing electromagnetic field distributions on the origin of color brain MRI images in order to estimate parameters such as electric field, power density, SAR, and hotspot regions. The results show that there is an extensive variety of electromagnetic field distributions in the

biological tissues, which highlights areas of high electrical field strength in regionalized areas that are essential for human safety. In spite of the statistic that the method is capable to deliver relative electromagnetic field values rather than absolute ones, it delivers valuable insight into spatial patterns of electromagnetic exposure. The method has the benefit of being suitable for informative uses, comparative analyses and initial safety assessments as well. Moreover, it is an important footstep in setting out the

groundwork for future research that will be devoted to standardizing electromagnetic simulations and assessing absolute fields.

There are several occurrences in which localized high-field regions are identified, highlighting the importance of using precautionary approaches when assessing electromagnetic exposure to these areas. Image-based EMF visualization can support awareness-driven safety evaluation and preliminary exposure analysis in medical imaging environments.

## REFERENCES

1. B. Pophof, *Health Phys.* **124** No 1, 39 (2023) <https://doi.org/10.1097/HP.0000000000001624>.
2. A.A. Oladipo, *J. Radiat. Res. Appl. Sci.* **18** No 4, 102010 (2025) <https://doi.org/10.1016/j.jrras.2025.102010>.
3. R. Zheng, *Brain Behav.* **13** No 6, e3004 (2023) <https://doi.org/10.1002/brb3.3004>.
4. P. Srinivas, *J. Nano-Electron. Phys.* **17** No 4, 04012 (2025) [https://doi.org/10.21272/jnep.17\(4\).04012](https://doi.org/10.21272/jnep.17(4).04012).
5. S. Chandrappa, *J. Nano-Electron. Phys.* **16** No 4, 04014 (2024) [https://doi.org/10.21272/jnep.16\(4\).04014](https://doi.org/10.21272/jnep.16(4).04014).
6. S. Chandrappa, *J. Nano-Electron. Phys.* **15** No 4, 04016 (2023) [https://doi.org/10.21272/jnep.15\(4\).04016](https://doi.org/10.21272/jnep.15(4).04016).
7. ICNIRP, *Health Phys.* **99** No 6, 818 (2010) <https://doi.org/10.1097/HP.0b013e31829e5580>.
8. ICNIRP, *Health Phys.* **118** No 5, 483 (2020) <https://doi.org/10.1097/hp.0000000000001210>.
9. P. Dimbylow, *Phys. Med. Biol.* **45** No 2, 383 (2000) <https://doi.org/10.1088/0031-9155/45/2/303>.

## Обчислювальна основа на медичних зображеннях для картографування електромагнітного поля та оцінки коефіцієнта питомого коефіцієнта поглинання (SAR) у біологічних тканинах

S. Chandrappa<sup>1</sup>, Prithviraj<sup>2</sup>, I.S. Rajesh<sup>3</sup> , K. Madhusudhana<sup>4</sup>, K.R. Sharath<sup>5</sup>, A. Pai<sup>6</sup>

<sup>1</sup> Department of Computer Science and Engineering (Data Science), Nagarjuna College of Engineering and Technology, Beedaganahalli Post, Devanahalli, Venkatagiri Kote, Bengaluru, India

<sup>2</sup> Department of Computer Science and Engineering, Nitte (Deemed to be University), NMAM Institute of Technology, Nitte, Karkala, India

<sup>3</sup> Department of Artificial Intelligence and Machine Learning, BMS Institute of Technology and Management, Bengaluru, India

<sup>4</sup> Department of Electronics & Communication Engineering, SDM Institute of Technology, Ujire, India

<sup>5</sup> Department of Computer Science and Engineering, Graphic Era (Deemed to be University), Dehradun, India

<sup>6</sup> MIT – School of Computing, MIT Art, Design and Technology University, Pune, Maharashtra, India

У всесвіті широко визнано, що магнітне випромінювання відіграє життєво важливу роль у сфері медичної візуалізації, такої як магнітно-резонансна томографія (МРТ), де радіочастотні електромагнітні поля, що випромінюються медичними інструментами, взаємодіють з тканинами біологічних об'єктів поблизу пристроїв. У цій дослідницькій роботі розглядається проблема, спричинена електромагнітними полями, та представлено підхід на основі зображень для розрахунку та оцінки розсіювання електромагнітного поля з використанням медичних зображень, отриманих за допомогою методу триангуляції. Було проведено дослідження зображень МРТ головного мозку, зібраних із загальнодоступного набору даних, і з використанням даних були створені нормалізовані поля карт інтенсивності електромагнітної енергії. На основі інформації, що міститься на цих картах, було розраховано розподіл радіочастотного магнітного поля, електричних полів, густини потужності та питомих коефіцієнтів поглинання (SAR). Пізніше було проведено дослідження на основі порогових значень, щоб знайти області з високими магнітними полями. Результати, отримані в результаті дослідження, встановлюють, що вплив електромагнітних полів на біологічні тканини є просторово неоднорідним, причому деякі області демонструють вищі рівні поглинання потоку та енергії. Важливо зазначити, що, хоча значення, отримані з даних, є відносними вимірюваннями, вони є достовірними з відомою поведінкою електромагнітного поля, що спостерігається в біологічних тканинах. В результаті запропонованої методології забезпечується практична та оперативна структура для оцінки та визначення радіаційного навантаження в середовищах медичної візуалізації.

**Ключові слова:** Електромагнітні поля, Оптичне випромінювання, МРТ, Коефіцієнт питомого амплітудного поглинання (SAR), Біологічні ефекти, Медична візуалізація.